PHYSICAL REVIEW A VOLUME 43, NUMBER 7 1 APRIL 1991

Quantum collapses and revivals in a nonlinear Jaynes-Cummings model

D. A. Cardimona, V. Kovanis,* M. P. Sharma,* and A. Gavrielides
Nonlinear Optics Center of Technology, Weapons Laboratory, Kirtland Air Force Base, New Mexico 87117
(Received 24 September 1990)

We investigate the atomic inversion dynamics when a multilevel atom interacts with a two-mode quantized radiation field in a Raman-type process. By utilizing the rotating-wave approximation and adiabatically eliminating all but two of the atomic levels, we derive a nonlinear-interaction Hamiltonian for this system. Working in the Schrödinger picture, we obtain numerical results that depend on the width and average photon number of the field statistics. Varying these photon statistics allows us to uncover secondary revivals that arise due to the complicated double sum over the two field modes that appear in the solutions. The origin of this phenomenon is described analytically.

I. INTRODUCTION

The system consisting of a two-level atom coupled, under the rotating-wave approximation, to a single quantized mode of the radiation field has come to be known in the quantum-optics literature as the Jaynes-Cummings model[1–4] (JCM) and is recognized as one of the few exactly solvable, fully quantum-mechanical models describing the interaction of matter with an electromagnetic field. Of particular interest is the case in which the field mode is initially prepared in the "most classical" quantum state, the coherent state (written as an infinite sum over a Poisson distribution of photon numbers).[5] Exact solutions describing the dynamical behavior of expectation values of variables such as the population inversion, the atomic dipole-correlation function, and the mean photon number can be obtained in this case in the form of an infinite series. In spite of the nearly classical nature of the initial state, the fact that the atom can act back on the single-mode quantum field, as predicted by the infinite-series solution, leads to dramatically different dynamics from that of its semiclassical analog. The most important example of this is the behavior of the population inversion. Instead of the steady Rabi oscillations of the inversion found in the case of a truly classical field coupled to the atom,[6] there is an initial collapse of these oscillations followed by regular revivals that slowly become broader and eventually overlap.[7] The net effect is eventually that of erratic, *though not chaotic,* oscillations of the inversion [see Fig. 8(c)]. The collapses occur because the many different components in the summation get out of phase. The revivals are a manifestation of the quantum nature of the electromagnetic field, which is mathematically reflected in the discrete summation.

Since the JCM is simple enough to yield many analytic results while still retaining enough complexity to be of very general interest, it has been an extremely popular theoretical model over the past three decades. It has been extended to include multimode fields,[8–16] multilevel atoms,[2,17,18] multiatom interactions,[19,20] and damping.[18,21] What makes all of these theoretical investigations of much more than academic interest are the exciting experimental results that have begun to appear. Single atoms have been isolated,[22] a single-mode two-photon Rydberg atom "micromaser"[23,24] has been made to operate in a high-Q cavity,[25] and the quantum collapse and revival for a single atom interacting with a single radiation mode may actually have been observed.[26]

Much attention has been focused on the collapse and revival phenomena in the Rabi oscillations of the population inversion because they provide evidence of the granularity of the radiation field.[2–4,7,27] The collapses and revivals have been described as arising from a kind of interference between the atom with classical field coupling and the atom with quantized cavity-mode coupling.[27] The overlapping and washing out of consecutive revivals is due to the incommensurate nature of the single-photon coupling energies ($\sim n^{1/2}$). If the JCM is extended to include two-photon coupling, then the possibility for commensurate energies arises [$\sim (n^{1/2})^2$].[8–16] Buck and Sukumar[8] indeed found exactly periodic collapses and revivals when they used the following intensity-dependent coupling Hamiltonian:

$$\hat{H}=\tfrac{1}{2}\omega_0\hat{\sigma}_z+\omega\hat{a}^{\dagger}\hat{a}+\lambda[(\hat{a}^{\dagger}\hat{a})^{1/2}\hat{a}^{\dagger}\hat{\sigma}^{-}+\hat{a}(\hat{a}^{\dagger}\hat{a})^{1/2}\hat{\sigma}^{+}]\ . \tag{1}$$

Phoenix and Knight[16] obtained the same results with their Raman-coupled Hamiltonian

$$\hat{H}=\tfrac{1}{2}\omega_0\hat{\sigma}_z+\omega\hat{a}^{\dagger}\hat{a}+\lambda\hat{a}^{\dagger}\hat{a}(\hat{\sigma}^{-}+\hat{\sigma}^{+})\ . \tag{2}$$

For both of these Hamiltonians the infinite series for the population inversion is exactly summable, due to the commensurate energies, and the exactly periodic solution is

$$\begin{aligned}W(t)&=-e^{-\langle n\rangle}\sum_{n=0}^{\infty}\frac{(\langle n\rangle)^n}{n!}\cos(2n\lambda t)\\&=-e^{-2\langle n\rangle\sin^2\lambda t}\cos(\langle n\rangle\sin 2\lambda t)\ .\end{aligned} \tag{3}$$

The phenomenological Hamiltonian for degenerate two-photon absorption

$$\hat{H}=\tfrac{1}{2}\omega_0\hat{\sigma}_z+\omega\hat{a}^{\dagger}\hat{a}+\lambda[(\hat{a}^{\dagger})^2\hat{\sigma}^{-}+(\hat{a})^2\hat{\sigma}^{+}] \tag{4}$$

also gives commensurate energies when the field is tuned from resonance by an amount equal to the coupling constant λ.[9,11,16] These nonlinear interaction Hamiltonians have sparked a great deal of theoretical interest in the extended JCM.[15,16,28]

In this paper we study the interaction of essentially a two-level atom interacting with a two-mode radiation field through a Raman interaction. We use a phenomenological Hamiltonian[15] very closely related to the Raman-coupled Hamiltonian of Phoenix and Knight[16] shown in Eq. (2). The dynamics we obtain for the level populations are nearly identical to those obtained by Gou[14] for a two-photon *absorption* interaction. By investigating the effects of varying the mean photon number of the photon distribution function used to describe the photon statistics of the fields, we uncovered what we call "secondary revivals" in the population dynamics that were unseen by Abdalla *et al.*[15] and unmentioned by Gou.[14] These secondary revivals arise due to the complicated interferences that occur in the *double* sum that appears in the calculation of the dynamics (summing over the photon distributions for *each* field mode). Our main mathematical contribution is to recognize that this double sum can be broken down into a series of Buck-Sukumar-like single sums, each of which can be summed to yield an overall envelope function as well as an oscillatory part whose phase difference from one sum to the next makes the origin of the secondary revivals obvious. A further contribution of this paper is to actually *derive* the phenomenological Hamiltonian used here using a method easily applied to the plethora of other phenomenological Hamiltonians used throughout the literature [e.g., Eqs. (1), (2), and (4)].

In the next section we introduce the phenomenological Hamiltonian for the Raman system under consideration in this paper and derive the fundamental observable, the population inversion, to be a double sum over the photon distributions for the two field modes. We then show how this double sum breaks up into a series of single Buck-Sukumar-like sums, which greatly illuminates the dynamics. In Sec. III we present numerical results for the population inversion given various initial photon distributions. Here we discover the secondary revivals. In Sec. IV we sum the population inversion series for two types of initial photon distributions. This allows us to provide an analytic explanation for the numerical observations of the preceding section. Section V is a summary and discussion of the results presented in this paper. We conclude with two appendices. Appendix A is the systematic derivation in the Schrödinger picture of the population inversion allowing for the detuning of the fields from the two-photon Raman resonance and for the dynamic Stark shifts of the atomic levels due to the applied fields.[12,24,29] Appendix B shows how the phenomenological Hamiltonian we use may be derived in the Heisenberg picture from the full Hamiltonian of Appendix A.

II. THE SYSTEM AND THE OBSERVABLE

The nonlinear process we consider in this paper is depicted in Fig. 1. Level $|1\rangle$ (at energy ω_1) (throughout this paper $\hbar=1$) is connected to level $|2\rangle$ (at energy ω_2) via a Raman interaction through the rest of the levels $|j\rangle$ (at energies ω_j). The pump radiation mode (ω_p) and the Stokes radiation mode (ω_S) are in two-photon resonance with the $|1\rangle$ to $|2\rangle$ transition ($\omega_p-\omega_S=\omega_2-\omega_1\equiv\omega_0$) and are far off resonance with the $|j\rangle$ states. We may easily write down a phenomenological rotating-wave-approximation Hamiltonian for this process as

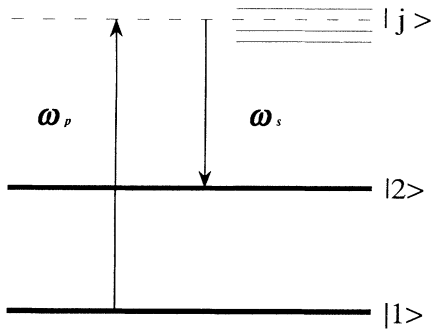

FIG. 1. This is the two-photon Raman process studied in the text. The pump field at ω_p and the Stokes field at ω_S allow resonant transitions to be made from state $|1\rangle$ to $|2\rangle$ through the off-resonant states $|j\rangle$.

$$\hat{H}=\tfrac{1}{2}\omega_0\hat{\sigma}_z+\omega_p\hat{a}_p^{\dagger}\hat{a}_p+\omega_S\hat{a}_S^{\dagger}\hat{a}_S+\lambda(\hat{a}_p^{\dagger}\hat{a}_S\hat{\sigma}^-+\hat{a}_p\hat{a}_S^{\dagger}\hat{\sigma}^+)\ , \tag{5}$$

where $\hat{\sigma}_z$ is the inversion operator and $\hat{a}_\alpha^{\dagger}(\hat{a}_\alpha)$ is the photon creation (annihilation) operator for mode α ($\alpha=p,S$). As discussed in Appendix B, this Hamiltonian ignores Stark shifts due to coupling through the virtual $|j\rangle$ levels. In the Schrödinger picture, we may write the system wave function to the same order of approximation as

$$|\Psi(t)\rangle=[P_p(n)P_S(m)]^{1/2}\times[C_1(t)|n,m,1\rangle+C_2(t)|n-1,m+1,2\rangle]\ , \tag{6}$$

where $P_\alpha(n)$ is the statistical distribution of photons in mode α.

The dynamics for this problem are obtained by using the time-dependent Schrödinger equation,

$$\hat{H}|\Psi(t)\rangle=i\frac{\partial}{\partial t}|\Psi(t)\rangle\ , \tag{7}$$

to derive the amplitude equations

$$\frac{\partial C_1(t)}{\partial t}=-i\lambda\sqrt{n(m+1)}C_2(t)\ , \tag{8a}$$

$$\frac{\partial C_2(t)}{\partial t}=-i\lambda\sqrt{n(m+1)}C_1(t), \tag{8b}$$

which are easily solved (for a more detailed discussion of this procedure, see Appendix A). The population inversion

$$W(t)=\langle\Psi(t)|\hat{\sigma}_z|\Psi(t)\rangle \tag{9a}$$

is then given by

$$W(t)=\sum_{n=0}^{\infty}\sum_{m=0}^{\infty}P(n)P(m)\cos[2\sqrt{n(m+1)}\lambda t] \quad (9b)$$

where the two modes have the same photon distribution.

The appearance of the complicated double sum tends to make one expect that the dynamics will be terribly involved and hard to sort out. However, if we rewrite Eq. (9b) as

$$\begin{aligned}W(t)=&\sum_{n=1}^{\infty}P(n)P(n-1)\cos(2n\lambda t)\\&+\sum_{n=0}^{\infty}P(n)P(n)\cos[2\sqrt{n(n+1)}\lambda t]\\&+\sum_{n=2}^{\infty}P(n)P(n-2)\cos[2\sqrt{n(n-1)}\lambda t]+\cdots ,\end{aligned} \quad (10)$$

we realize that the complicated double sum of Eq. (9b) consists essentially of an infinite collection of sums that each individually behaves almost like the exactly periodic degenerate-mode case studied by Buck and Sukumar.[8–10] Because of the commensurate nature of the energies involved in the Buck-Sukumar dynamics and the fact that the nondegenerate-mode problem being studied here is merely a series of Buck-Sukumar-like sums, some of the periodicity inherent in that model should manifest itself in this problem. As we will discover in the next section, this is indeed the case

III. NUMERICAL RESULTS WITH COMPUTER GRAPHICS

In Figs. 2–4 we plot the inversion [Eq. (9b) or (10), since they are equivalent] with the corresponding statistical distribution used. From these figures, the periodicity inherent in the Buck-Sukumar-type problem (intensity-dependent Hamiltonians) is obvious. In Figs. 2 and 3 we use the normalized Gaussian

$$P(n)=\frac{\exp[-(n-\langle n\rangle)^2/2\Gamma^2]}{\sum_n \exp[-(n-\langle n\rangle)^2/2\Gamma^2]} \quad (11)$$

for the photon distribution function, with $\Gamma=3$ (Fig. 2) or 6 (Fig. 3). This distribution is chosen for the convenience it affords in the choice of width (Γ) and mean ($\langle n\rangle$). In Fig. 4 we use the normalized Poisson distribution

$$P(n)=e^{-\langle n\rangle}\frac{\langle n\rangle^n}{n!} . \quad (12)$$

This distribution is more physical in that it is the distribution followed by photons in a coherent state, however its width is intimately related to its mean ($\Gamma\sim\langle n\rangle^{1/2}$). In each of these figures, $\langle n\rangle$ takes on the values of 5, 10, 20, and 40.

In Fig. 2 notice that as $\langle n\rangle$ decreases, a "secondary revival" begins to appear at later times, and moves to earlier times as $\langle n\rangle$ continues to decrease. In Fig. 3, where the width is double that of Fig. 2, the dynamics are a bit more complicated. On either side of where the secondary revival would have appeared for a narrower distribution, two revivals appear. Also, these new revivals appear at much earlier times for a given $\langle n\rangle$. In Fig. 4 the dynamics are not nearly as clean as in the Gaussian cases due to the changing width as $\langle n\rangle$ changes. However, the trends as illuminated through the use of the Gaussian, where the effects of changing $\langle n\rangle$ are clearly separate from the effects of changing width, are still valid.

If we allow detuning from the two-photon resonance in our interaction, we may use the population inversion derived in Appendix A. The effect of detuning is twofold. First, being off resonant, the probability for transferring population from state $|1\rangle$ to state $|2\rangle$ through the two-photon transition becomes smaller. This causes the population inversion to have an average less than zero (instead of zero as it is when detuning is zero as in the figures). Second, the presence of detuning essentially changes the time scale such that the duration of every collapse and revival is lengthened.

IV. EXACTLY SOLVABLE MODEL (DOUBLY SUMMING THE DOUBLE SUM)

For simplicity, let us consider the double sum

$$\sum_{n=0}^{\infty}\sum_{m=0}^{\infty}P(n)P(m)\cos(2\sqrt{nm}\,\lambda t) . \quad (13)$$

In all of its essentials this will be identical to the double sum of Eq. (9b). If we break this sum up into a series of single sums as in Eq. (10), we may write

$$\begin{aligned}\sum_{n=0}^{\infty}\sum_{m=0}^{\infty}P(n)P(m)\cos(2\sqrt{nm}\,\lambda t)=&\sum_{n=0}^{\infty}P(n)P(n)\cos(2n\lambda t)+\sum_{n=0}^{\infty}P(n)P(n+k)\cos[2\sqrt{n(n+k)}\lambda t]\\&+\sum_{n=k}^{\infty}P(n)P(n-k)\cos[2\sqrt{n(n-k)}\lambda t] ,\end{aligned} \quad (14)$$

where $k=1,2,3,\ldots$. The first term we will call the zeroth diagonal sum and the sums with $\pm k$ we will call the $\pm k$th diagonal sums.

The zeroth diagonal sum for the case of a common Poisson can be summed exactly to give

$$\begin{aligned}W_d(t)=&\sum_{n=0}^{\infty}e^{-2\langle n\rangle}\frac{(\langle n\rangle)^{2n}}{(n!)^2}\cos(2n\lambda t)\\=&\tfrac{1}{2}e^{-2\langle n\rangle}[I_0(2Z)+I_0(2Z^*)] ,\end{aligned} \quad (15)$$

where $Z=\langle n\rangle\exp(i\lambda t)$ and $I_0(x)$ is the zeroth-order

modified Bessel function. This solution is very reminiscent of the Buck-Sukumar result [see Eq. (3)]

$$W_{\mathrm{BS}}(t)=\sum_{n=0}^{\infty} e^{-\langle n\rangle}\frac{(\langle n\rangle)^n}{n!}\cos(2n\lambda t)$$
$$=\tfrac{1}{2}e^{-\langle n\rangle}(e^{z}+e^{z^*}) , \tag{16}$$

where $z=\langle n\rangle\exp(i2\lambda t)$.

This expression is interesting and has a nice analogy with the corresponding Buck-Sukumar result, but it does not lend itself to easy interpretation. A more transparent solution may be obtained if we let

$$P(n)=N[e^{-\langle n\rangle}(\langle n\rangle)^n/n!]^{1/2} , \tag{17a}$$

where N, the norm, is given by

$$N=\frac{1}{\sum_{n=0}^{\infty}[e^{-\langle n\rangle}(\langle n\rangle)^n/n!]^{1/2}} . \tag{17b}$$

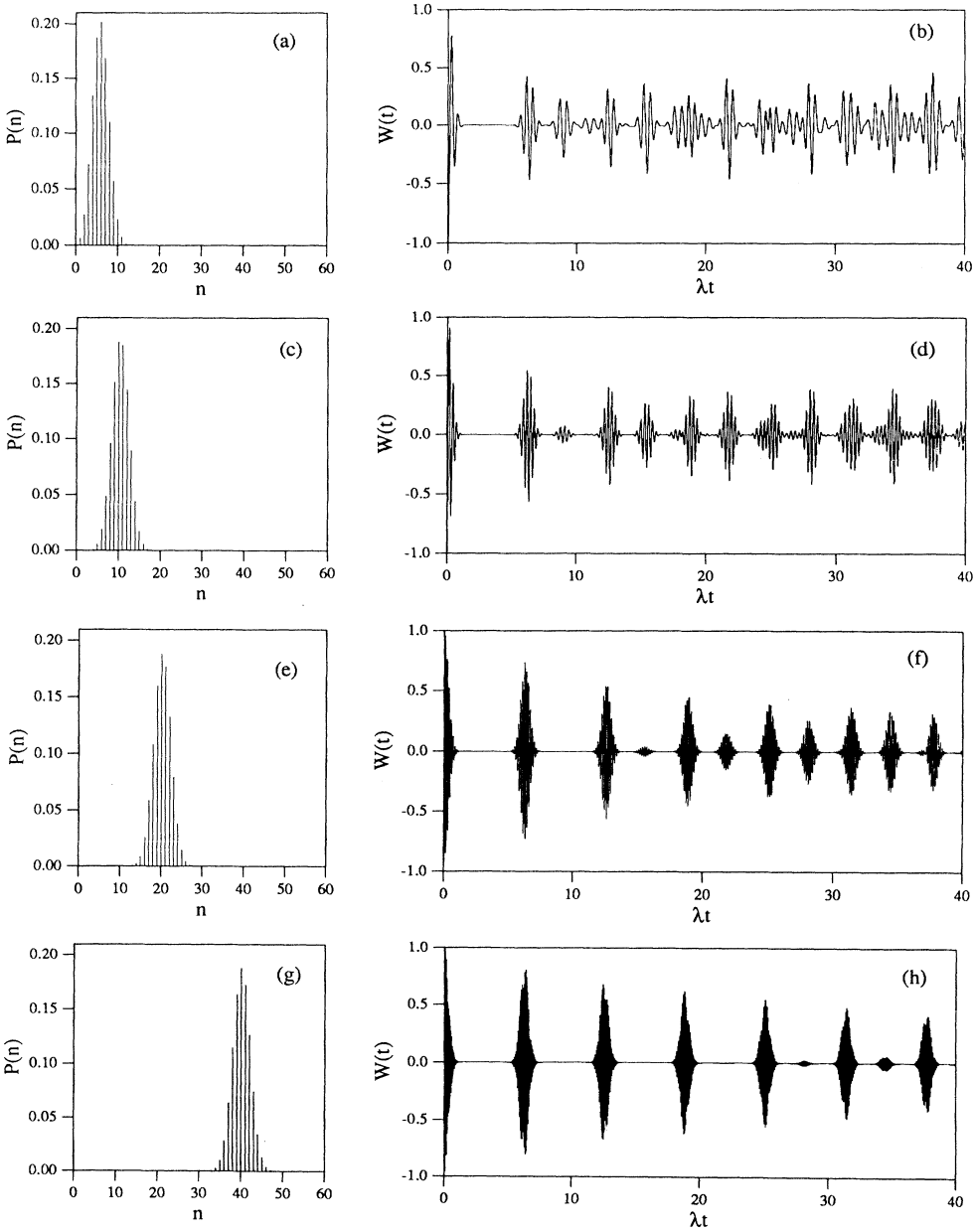

FIG. 2. This shows the emergence of the *"secondary revivals"* described in the text. We plot the dynamics of the population inversion $W(t)$ vs the dimensionless time λt, with λ the coupling constant shown in Eq. (5), along with the initial photon distributions that led to those dynamics. The distributions are Gaussian with width $\Gamma=3$ $(\lambda\,\mathrm{sec})^{-1}$ and mean $\langle n\rangle=5$ (a), (b), 10 (c), (d), 20 (e), (f), and 40 (g), (h).

Then we find the zeroth diagonal sum to be

$$\sum_{n=0}^{\infty} P^2(n)\cos(2n\lambda t)=N^2e^{-\langle n\rangle}\sum_{n=0}^{\infty}\frac{(\langle n\rangle)^n}{n!}\cos(2n\lambda t) \tag{18a}$$

$$=N^2e^{-2\langle n\rangle\sin^2(\lambda t)} \times\cos[\langle n\rangle\sin(2\lambda t)]\ . \tag{18b}$$

For $\langle n\rangle \gg 1$, contributions to the various sums will occur only for large n, so in the $\pm k$th diagonal sums we may approximate $P(n)P(n\pm k)$ $(k \ll \langle n\rangle)$ as $P^2(n)$ and the cosines as

$$\cos 2\sqrt{n(n\pm k)}\lambda t \approx \cos 2n\left[1\pm\frac{k}{2n}-\frac{k^2}{8n^2}\right]\lambda t \approx \cos\left[2n\pm k-\frac{k^2}{4\langle n\rangle}\right]\lambda t\ . \tag{19}$$

We can now sum the $\pm k$th diagonal series to get the

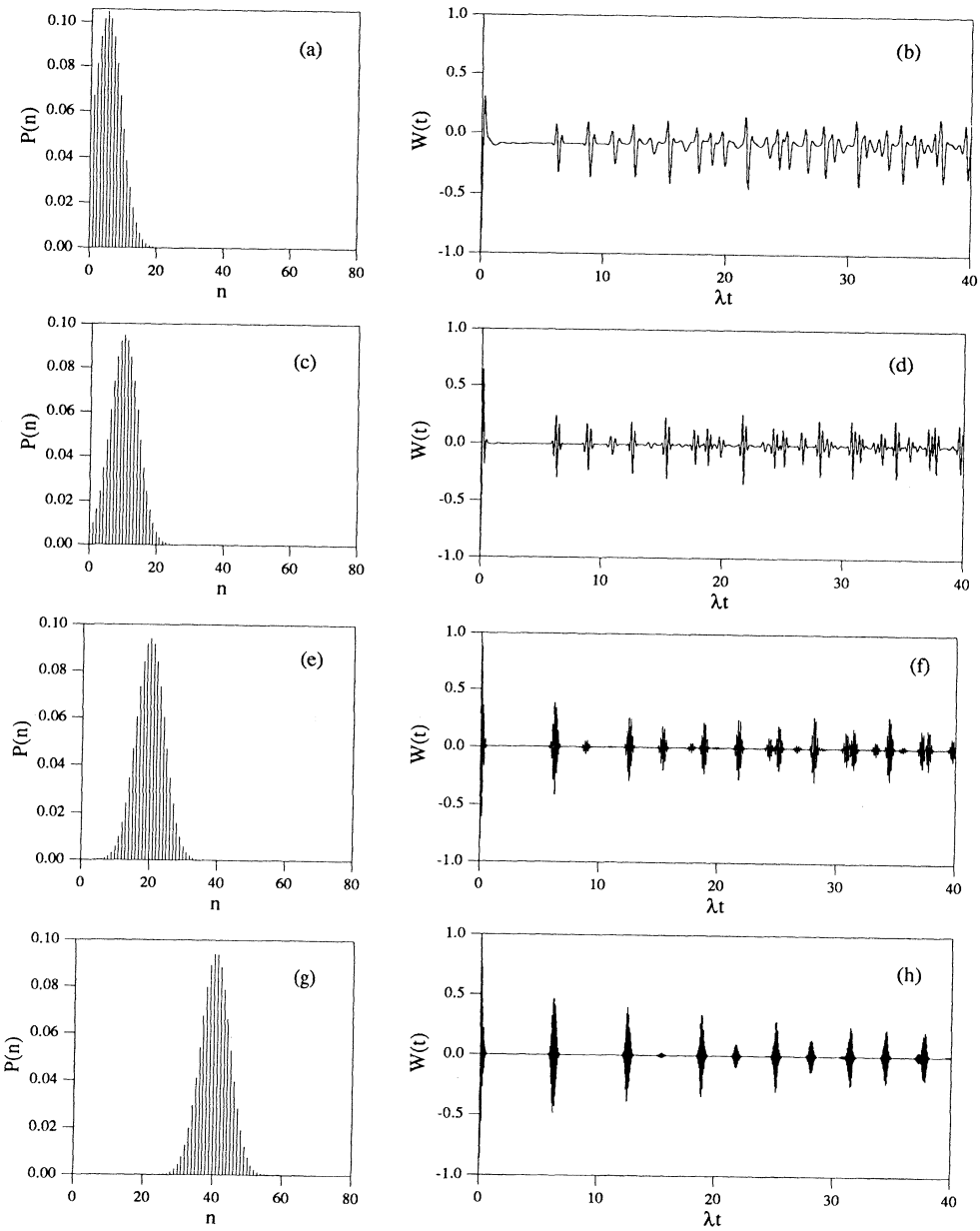

FIG. 3. This shows the effects of increasing the width of the initial photon distribution. Everything is the same here as in Fig. 2, except that the width $\Gamma=6\,(\lambda\,\mathrm{sec})^{-1}$.

$\pm k$th diagonal sum

$$\approx N^2 e^{-2\langle n\rangle \sin^2\lambda t} \times \cos\left[\langle n\rangle \sin 2\lambda t + k\lambda t\left[\pm 1 - \frac{k}{4\langle n\rangle}\right]\right]. \quad (20)$$

Notice that each of these diagonal sums has the same Buck-Sukumar envelope $[\exp(-2\langle n\rangle \sin^2\lambda t)]$, but that the oscillating parts of the $\pm k$th diagonal sums are phase shifted by $k\lambda t(\pm 1 - k/4\langle n\rangle)$ from the zeroth diagonal sum. The envelope maximizes when $\lambda t = N\pi$. At these peaks, the kth diagonal sum is about $k\lambda t = kN\pi$ out of phase with the zeroth diagonal sum. That is, the first diagonal sum ($k=1$) is $N\pi$ out of phase with the zeroth diagonal sum at each peak and so they constructively (destructively) interfere at the first, third, fifth, . . . (second, fourth, sixth, . . .) peaks. The second diagonal sum ($k=2$) is $2N\pi$ out of phase with the zeroth diagonal sum at each peak, i.e., they are *in* phase at *every* peak and so constructively interfere. Likewise for the rest of the $\pm k$th diagonal sums. So, we see that there will be a pairwise cancellation at every other peak. This cancellation process will break down when the phase shift is not "near

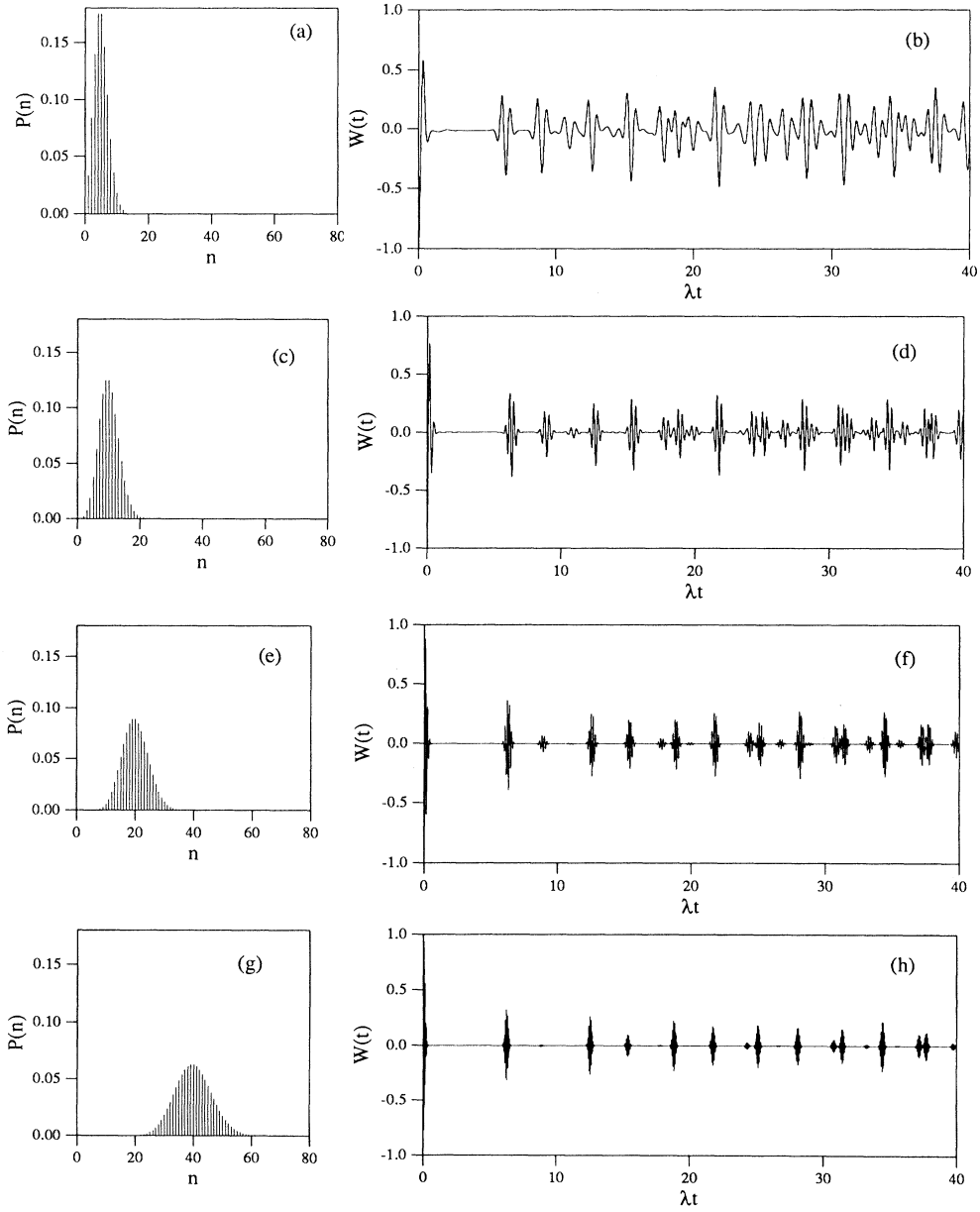

FIG. 4. This demonstrates the differences between the artificial Gaussian initial photon distributions of Figs. 2 and 3 and the more physical Poisson distribution. Again the parameters are the same as in Figs. 2 and 3, except here the width varies as $\langle n\rangle^{1/2}$.

enough" to a multiple of π. Roughly, we argue as follows. Let $\lambda t = N\pi$. Then the phase shift is

$$k\lambda t\left[\pm 1-\frac{k}{4\langle n\rangle}\right]=kN\pi\left[\pm 1-\frac{k}{4\langle n\rangle}\right]$$

$$=\pm kN\pi-\frac{k^2N\pi}{4\langle n\rangle}\ . \tag{21}$$

This will be "different enough" from a multiple of π when

$$\frac{k^2N}{4\langle n\rangle}\geq x \tag{22a}$$

(where x is some "small" number),

$$N\geq\frac{4x}{k^2}\langle n\rangle\ , \tag{22b}$$

$$N_{\max}\geq 4x\langle n\rangle\ . \tag{22c}$$

From the graphs we see that for $\langle n\rangle\sim 10$, $N_{\max}\sim 3$ and we estimate x to be on the order of 0.05. Therefore when $\lambda t\geq 0.2\pi\langle n\rangle$ the cancellation process begins to fail and we see the appearance of the "secondary revivals."

We can now specify the revival times involved in the double-sum solution for this two-photon process. As described above, due to the pairwise cancellations that occur the time for the primary revival to occur is when λt is an even multiple of π, i.e., the primary revival times are

$$\tau_1=2m\pi/\lambda,\quad m=1,2,3,\ldots\ . \tag{23}$$

When the cancellation process begins to fail, the secondary revival begins to appear when λt is near the odd multiple of π closest to $0.2\langle n\rangle$ (see the discussion just prior to this paragraph), i.e., the secondary revival times are

$$\tau_2=([0.2\langle n\rangle]_{\text{odd}}+2m)\pi/\lambda,\quad m=0,1,2,\ldots \tag{24}$$

where $[x]_{\text{odd}}$ is the odd integer closest to x.

Now that we have an intuitive feeling for what is happening in the dynamics, let us return to the expression derived using the more physical Poisson distribution, Eq. (15). If we let $2Z=X+iY$ and use the integral representation of I_0, we may rewrite Eq. (15) as

$$W_d(t)=e^{-2\langle n\rangle}\mathrm{Re}[I_0(X+iY)] \tag{25a}$$

$$=e^{-2\langle n\rangle}\mathrm{Re}\left[\frac{1}{\pi}\int_0^{\pi}e^{\pm(X+iY)\cos\theta}d\theta\right] \tag{25b}$$

$$=e^{-2\langle n\rangle}\frac{1}{\pi}\int_0^{\pi}e^{\pm X\cos\theta}\cos(Y\cos\theta)d\theta\ . \tag{25c}$$

Since we now expect maxima to occur around $\lambda t=N\pi$, let us look there. In that case we have

$$Y=2\langle n\rangle\sin\lambda t\approx 0\ , \tag{26}$$

and

$$W_d(\lambda_t\approx N\pi)\approx e^{-2\langle n\rangle}\frac{1}{\pi}\int_0^{\pi}e^{\pm X\cos\theta}d\theta \tag{27a}$$

$$=e^{-2\langle n\rangle}I_0(2\langle n\rangle\cos\lambda t)\ . \tag{27b}$$

We expect minima near $\lambda t=(2N+1)\pi/2$, so let us look there now. Then we have

$$Y\approx\pm 2\langle n\rangle \tag{28a}$$

$$X=2\langle n\rangle\cos\lambda t\approx 0\ , \tag{28b}$$

and therefore

$$W_d[\lambda t\approx(2N+1)\pi/2]\approx e^{-2\langle n\rangle}\frac{1}{\pi}\int_0^{\pi}\cos(2\langle n\rangle\cos\theta)d\theta \tag{29a}$$

$$=e^{-2\langle n\rangle}J_0(2\langle n\rangle)\ . \tag{29b}$$

For $\langle n\rangle\gg 1$,

$$e^{-2\langle n\rangle}J_0(2\langle n\rangle)\rightarrow 0 \tag{29c}$$

and we may write the approximate envelope E in the case when $P(n)$ is a Poisson distribution as the sum of Eqs. (27b) and (29c)

$$E(W_d(\lambda t))\approx e^{-2\langle n\rangle}I_0(2\langle n\rangle\cos\lambda t)\ . \tag{30}$$

For the $\pm k$th diagonal sums we may expand the $[n(n\pm k)]^{1/2}$ as we did when the photon distribution was a square root of a Poisson function [see Eq. (19)] and find the contributions to the population inversion for a Poisson distribution to be

$$W_{\pm k}(\lambda t)=e^{-2\langle n\rangle}\frac{1}{\pi}\times\int_0^{\pi}e^{\pm X\cos\theta}[\cos(Y\cos\theta)\cos(k\lambda t)\mp\sin(Y\cos\theta)\sin(k\lambda t)]d\theta\ . \tag{31}$$

Again looking near $\lambda t=N\pi$ we find

$$W_{\pm k}(\lambda t\approx N\pi)\approx(-1)^{kN}e^{-2\langle n\rangle}I_0(2\langle n\rangle\cos\lambda t)\ , \tag{32}$$

and for $\lambda t\approx(2N+1)\pi/2$ we find [for $m=k(2N+1)$]

$$W_{\pm k}[\lambda t\approx(2N+1)\pi/2]\approx e^{-2\langle n\rangle}J_0(2\langle n\rangle)\cos(m\pi/2) \tag{33a}$$

$$\rightarrow 0,\quad \langle n\rangle\gg 1\ . \tag{33b}$$

Therefore, as for Eq. (30), we add Eqs. (32) and (33b) to obtain the approximate envelope function E for the $\pm k$th diagonal sum in the case of a Poisson distribution function to be

$$E(W_{\pm k}(\lambda t))\approx(-1)^{kN}e^{-2\langle n\rangle}I_0(2\langle n\rangle\cos\lambda t)\ , \tag{34}$$

with $N=0,1,2,\ldots$. Just as for the case when we used a square root of a Poisson function [see Eq. (20)], we again find the same constructive (destructive) interference effect between neighboring sums near $\lambda t\approx N\pi$ for $kN=0,2,4,\ldots$ $(1,3,5,\ldots)$.

In Fig. 5 we compare the Gaussian, the Poisson, and the square root of a Poisson distributions and their resulting dynamics for $\langle n\rangle=15$. The Gaussian has $\Gamma=6$ so that it is nearly identical to the Poisson, but the square root of a Poisson is obviously wider (its width goes like

$\sqrt{2}$ times the width of the normal Poisson). Other than the width, there is no qualitative difference between any of these distributions.

In Fig. 6(a) we compare the two envelope functions found above [the Buck-Sukumar envelope of Eq. (18c) or Eq. (20) and the Bessel function envelope of Eq. (30) or Eq. (34)]. It is obvious that the two are nearly identical, even though the initial photon probability distributions were different. The $N\pi$ periodicity is inherent in the two-photon process and does not depend strongly on initial conditions. In Fig. 6(b) the effect of the Buck-Sukumar envelope function is graphically made obvious, while in Fig. 7 the cancellation effect between the first two diagonal sums is represented (along with the full sum of all of the diagonal sums).

V. SUMMARY AND DISCUSSION

In this paper we have studied the dynamics of the population inversion of a nonlinear Jaynes-Cummings Hamiltonian that describes Raman processes. We derived the population inversion to be a complicated-looking double

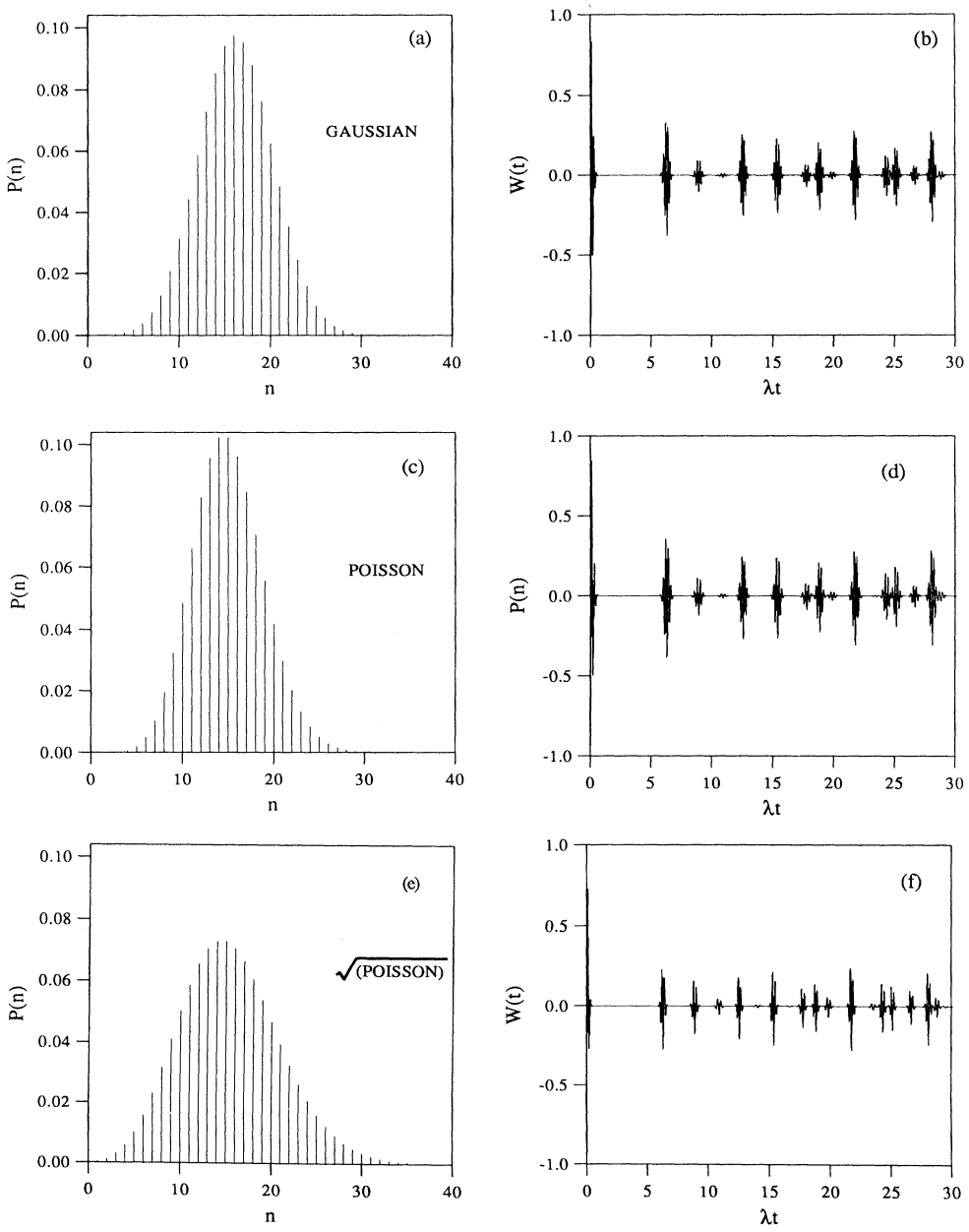

FIG. 5. Here we show that the artificial square root of a Poisson photon distribution, introduced in the text in order to obtain some analytic intuition into the origin of the secondary revivals, is not qualitatively different from the other distributions used. We use $\langle n \rangle = 15$ and for (a) $\Gamma = 6\ (\lambda\ \mathrm{sec})^{-1}$.

sum, but we were able to simplify the description of the dynamics by rearranging the double sum into a series of "simple" single sums that have a strong resemblance to the Buck-Sukumar model.

With the help of an artificial Gaussian distribution for the initial photon occupation, we were able to map out the essential dynamics as a function of width separate from the mean and vice versa. Note that the Gaussian is an excellent limit of the Poisson for large average quantum numbers. For relatively narrow widths we numerically observed the emergence of secondary revivals, while for wider distributions we noticed the appearance of tertiary revivals. These new revivals showed up late in the dynamics for large average n and moved to earlier times as $\langle n \rangle$ was decreased.

The main mathematical contribution of this paper is the summing of the double sum when the initial photon distribution is either a Poisson or the square root of a Poisson, and the subsequent explanation of the origin of the new secondary revivals. By utilizing the square root

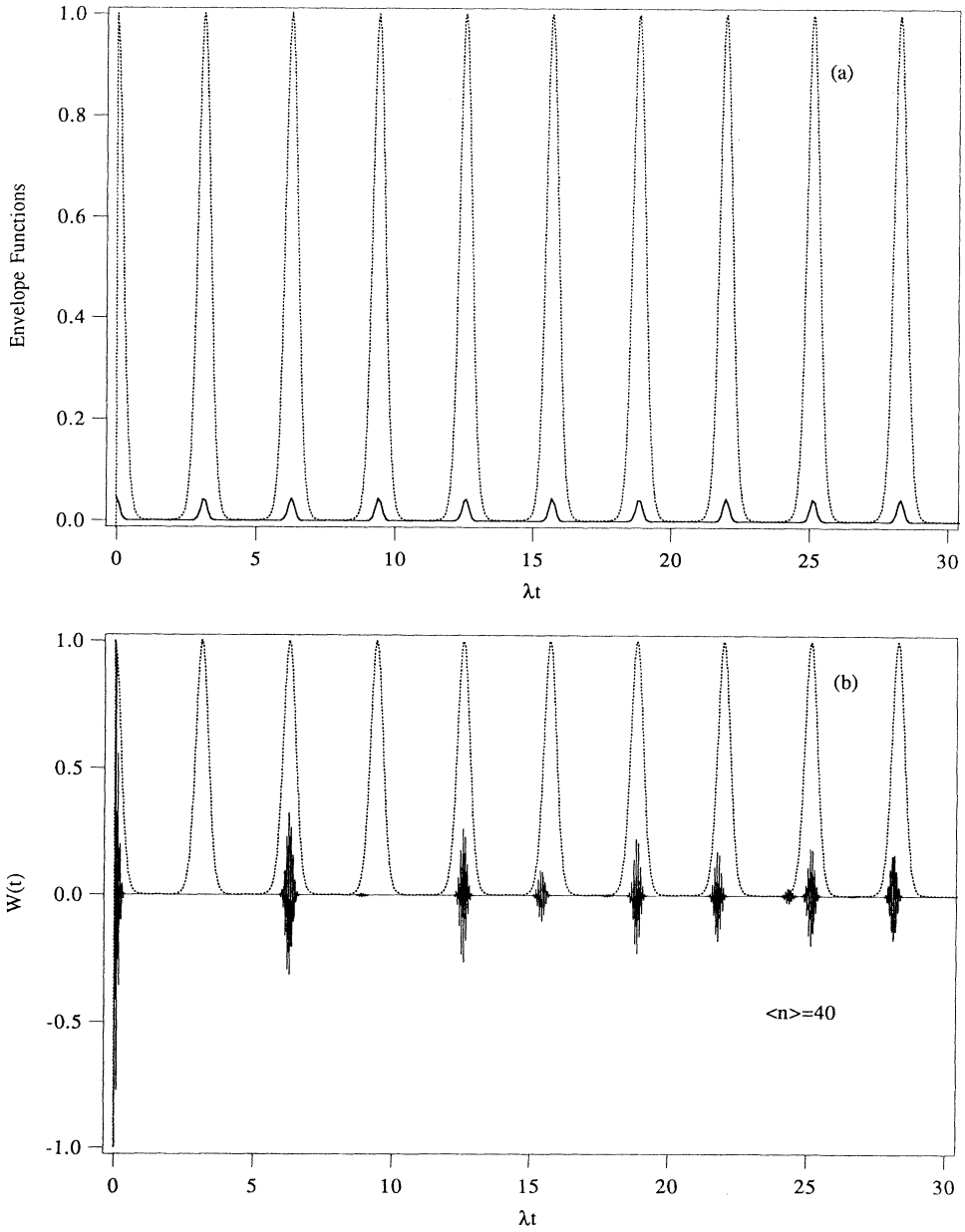

FIG. 6. Here we plot the envelope functions common to each of the diagonal sums of Sec. IV, for $\langle n \rangle = 40$. In (a) we compare the envelope for a Poisson photon distribution (solid line), $e^{-2\langle n \rangle} I_0(2\langle n \rangle \cos\lambda t)$, with the envelope for a square root of a Poisson distribution (dotted line), $\exp(-2\langle n \rangle \sin^2\lambda t)$ [if we included the $(N)^2$ factor in front of this envelope the dotted line would be indistinguishable from the solid line]. In (b) we plot the total sum of all the diagonal contributions (i.e., the total population inversion) (solid line) along with the envelope $\exp(-2\langle n \rangle \sin^2\lambda t)$ (dotted line) in order to show the origin of the surprising order found in the complicated double sum.

of a Poisson, we were able to analytically derive an expression for the envelope functions and the relative phases between each of the single sums. We were able to pinpoint the origin of the secondary revivals as arising from the phase difference between the neighboring sums. Breaking the double sum into a series of single Buck-Sukumar-like sums, we noticed that the secondary revivals are actually always present, but that the superposition of the single sums resulted in the appropriate interference (constructive or destructive) at every other revival position. The position of the interference was made clear by the analytic determination of the relative phases. With these interference positions known, the revival times become obvious. The primary revival times occur at even multiples of π/λ and the secondary revival times start near the first odd multiple of π/λ closest to $0.2\langle n \rangle$ and then continue at every odd multiple of π/λ after that. Notice that the first secondary revival occurs at a time that is directly proportional to $\langle n \rangle$.

The essence of this paper is summarized in Fig. 8 where we compare the Buck-Sukumar model (BSM) and the standard Jaynes-Cummings model to the model under investigation here. Notice that the only similarity that all three models possess is quantum collapses and revivals. The BSM sustains these forever due to the commensurability of its energy spectrum (linear in n), while the other two models dephase after a certain amount of time due to their incommensurate energy spectrum (going as the

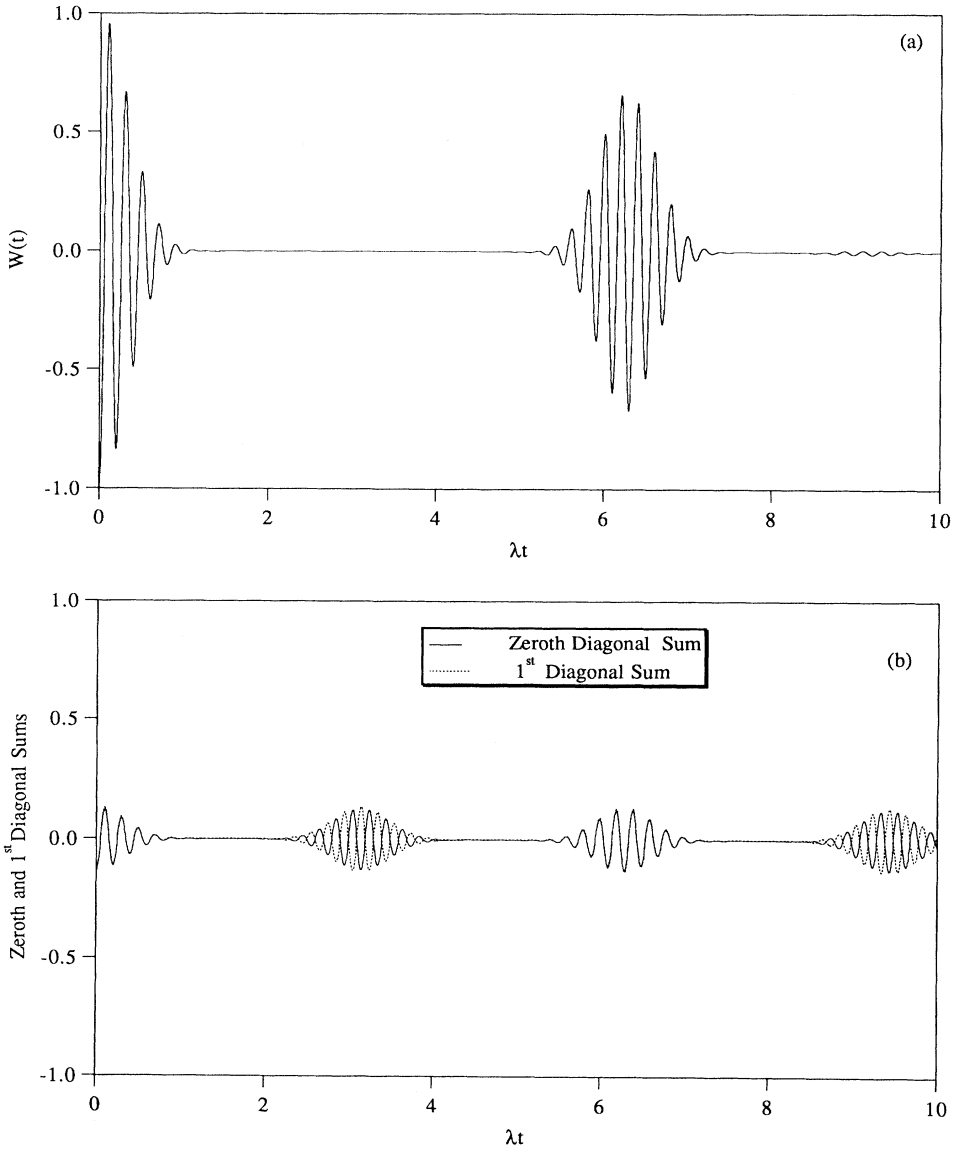

FIG. 7. The 180° phase shift between the various diagonal sums at every other peak in the envelope function of Fig. 6 is demonstrated here. In (a) the total double sum in the population inversion is shown for a Gaussian photon distribution with $\Gamma=3\ (\lambda\,\mathrm{sec})^{-1}$ and $\langle n \rangle = 15$. In (b) the zeroth diagonal sum (solid) and the first diagonal sum (dotted) are plotted together. The time is again in units of λ.

square root of the quantum number). For the same average photon number, the standard JCM becomes erratic much sooner than the present model. The spectrum of our model is *effectively* linear in quantum number (for a large average number of photons in the initial distribution) due to the two-photon nature of the problem, as we noticed when we broke the double sum into a series of BSM-like single sums. This explains why the dynamics of this model retain their collapse and revival structure for a much longer time than the standard JCM. This kind of commensurability is a lucky accident only when two-quanta exchanges are involved (such as in two-photon absorption processes or Raman processes). In these cases, the square root that comes from the quantization of the radiation field is nullified, allowing the energy spectrum to become linear.

Preliminary results of this research have been presented.[30] The effect of the dynamic Stark shift and other types of initial photon distributions are under investigation now and will be presented elsewhere.

Note added in proof. C. C. Gerry and J. H. Eberly [Phys. Rev. A **42**, 6805 (1990)] have seen the secondary revivals observed here, but did not explain their origin.

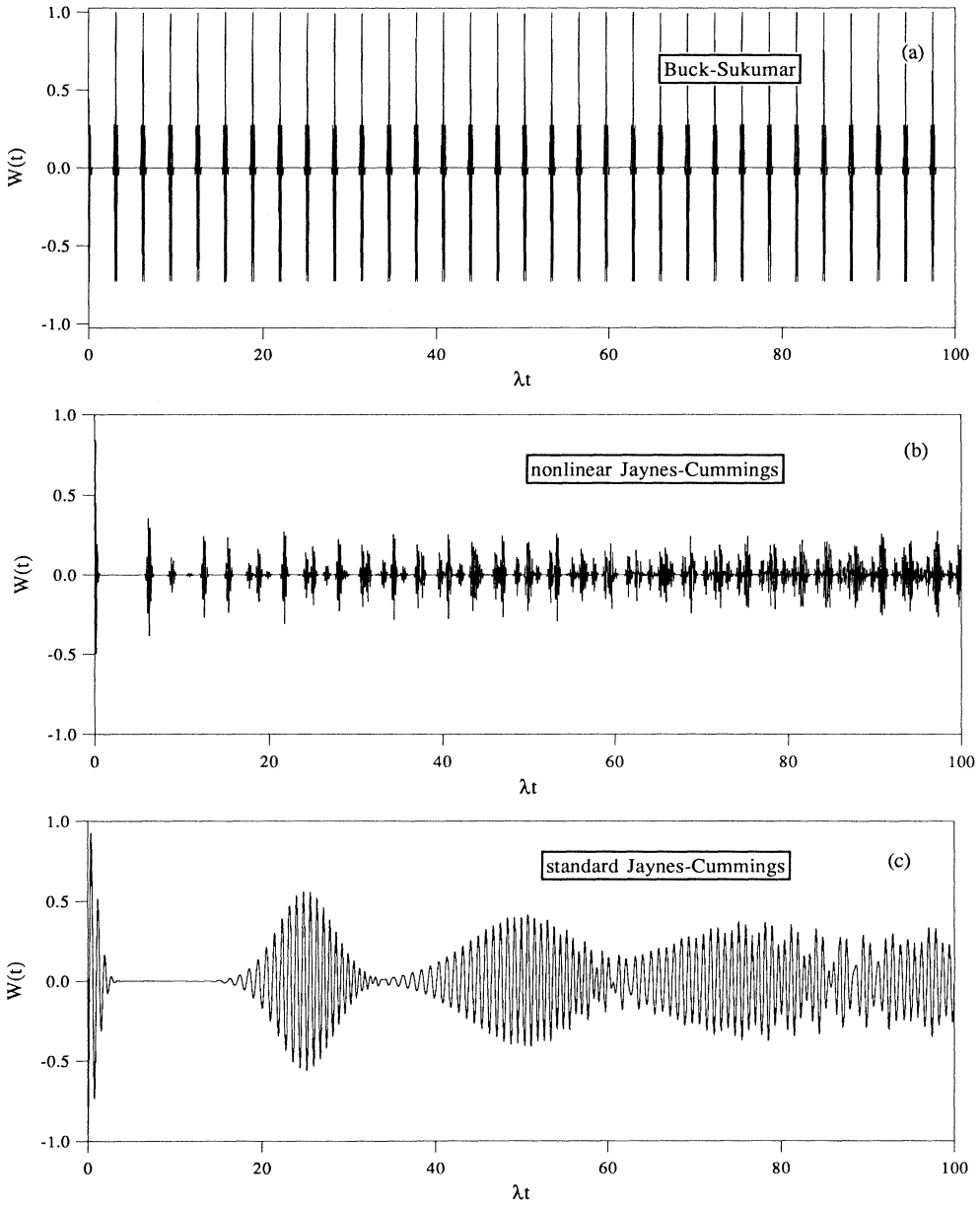

FIG. 8. Here the population inversion dynamics are contrasted and compared for (a) a *degenerate* two-photon process (the Buck-Sukumar model), (b) a *nondegenerate* two-photon process (the nonlinear Jaynes-Cummings model studied in this paper), and (c) a one-photon process (the standard Jaynes-Cummings model). In each case a Poisson photon distribution with $\langle n \rangle = 15$ is used.

APPENDIX A: ATOMIC DYNAMICS IN THE SCHRÖDINGER PICTURE

The system shown in Fig. 1 may be described by the Hamiltonian (with $\hbar=1$)

$$\hat{H}=\omega_1\hat{\sigma}_{11}+\omega_2\hat{\sigma}_{22}+\sum_j\omega_j\hat{\sigma}_{jj}+\omega_1\hat{a}_p^{\dagger}\hat{a}_p+\omega_2\hat{a}_S^{\dagger}\hat{a}_S-\hat{\mathbf{d}}\cdot\hat{\mathbf{E}}\ , \tag{A1}$$

where $\hat{\sigma}_{ij}=|i\rangle\langle j|$ is the atomic transition operator, $\hat{a}_\alpha^{\dagger}(\hat{a}_\alpha)$ is the creation (annihilation) operator for the αth radiation mode ($\alpha=p,S$), $\hat{\mathbf{d}}$ is the dipole moment operator,

$$\hat{\mathbf{d}}=\sum_j(\mathbf{d}_{1j}\hat{\sigma}_{1j}+\mathbf{d}_{2j}\hat{\sigma}_{2j}+\mathbf{d}_{j1}\hat{\sigma}_{j1}+\mathbf{d}_{j2}\hat{\sigma}_{j2})\ , \tag{A2}$$

and $\hat{\mathbf{E}}$ is the electric field operator. $\hat{\mathbf{E}}$ may be written for a two-mode field as

$$\hat{\mathbf{E}}=iA_p(\boldsymbol{\epsilon}_p\hat{a}_p-\boldsymbol{\epsilon}_p\hat{a}_p^{\dagger})+iA_S(\boldsymbol{\epsilon}_S\hat{a}_S-\boldsymbol{\epsilon}_S\hat{a}_S^{\dagger})\ , \tag{A3}$$

where $A_\alpha=(2\pi\omega_\alpha/V_\alpha)^{1/2}$ (V_α is the quantization volume for mode α) and $\boldsymbol{\epsilon}_\alpha$ is the unit polarization vector for mode α. Working in the Schrödinger picture, we write the system wave function for Raman scattering as

$$|\Psi(t)\rangle=e^{-i(n\omega_p+m\omega_S+\omega_1)t}[P_p(n)P_S(m)]^{1/2}\times\left[C_1(t)|n,m,1\rangle+C_2(t)|n-1,m+1,2\rangle e^{i\Delta t}+\sum_j C_j(t)|n-1,m,j\rangle e^{i\Delta_j t}\right]\ , \tag{A4}$$

where $P_\alpha(n)$ is the statistical distribution of photons in mode α, $\Delta=\omega_p-\omega_S-(\omega_2-\omega_1)$, and $\Delta_j=\omega_p-(\omega_j-\omega_1)$.

Schrödinger's time-dependent wave function [Eq. (7)] yields the following set of differential equations for the slowly varying amplitudes in the rotating-wave approximation (RWA)

$$\frac{\partial C_1(t)}{\partial t}=\sum_j\Omega_{jp}C_j(t)e^{i\Delta_j t}\ , \tag{A5a}$$

$$\frac{\partial C_2(t)}{\partial t}=\sum_j\Omega_{jS}C_j(t)e^{i(\Delta_j-\Delta)t}\ , \tag{A5b}$$

$$\frac{\partial C_j(t)}{\partial t}=-\Omega_{jp}^*C_1(t)e^{-i\Delta_j t}-\Omega_{jS}^*C_2(t)e^{-i(\Delta_j-\Delta)t}\ , \tag{A5c}$$

where the Rabi frequencies[6] are

$$\Omega_{jp}=\mathbf{d}_{1j}\cdot\boldsymbol{\epsilon}_p^*\sqrt{n}\,A_p\ , \tag{A6a}$$

$$\Omega_{jS}=\mathbf{d}_{2j}\cdot\boldsymbol{\epsilon}_S^*\sqrt{m+1}\,A_S\ . \tag{A6b}$$

Since we are interested in Raman scattering in which the intermediate states $|j\rangle$ are far off resonance ($\Delta_j\gg\Delta$), we may adiabatically eliminate these virtual state amplitudes.[12,31–33] Following Ref. 32 we integrate Eq. (A5c) formally and adiabatically approximate the resulting integrals by dropping terms of the order of $[dC_1(t)/dt]/\Delta_j$ or $[dC_2(t)/dt]/\Delta_j$ to obtain

$$C_j(t)e^{i\Delta_j t}\approx-i\frac{\Omega_{jp}^*}{\Delta_j}C_1(t)[1-C_1(0)e^{i\Delta_j t}]-i\frac{\Omega_{jS}^*}{\Delta_j-\Delta}C_2(t)[1-C_2(0)e^{i(\Delta_j-\Delta)t}]\ . \tag{A7}$$

If we substitute this back into Eqs. (A5a) and (A5b) and drop terms oscillating rapidly at frequency Δ_j (in the spirit of the RWA), we will introduce the Stark shifts of the levels[29,33]

$$S_1\equiv\sum_j|\Omega_{jp}|^2/\Delta_j\ , \tag{A8a}$$

$$S_2\equiv\sum_j|\Omega_{jS}|^2/(\Delta_j-\Delta)\ , \tag{A8b}$$

as well as the two-photon Rabi frequency[31–33]

$$R\equiv\sum_j\frac{\Omega_{jp}\Omega_{jS}^*}{\Delta_j}\ . \tag{A8c}$$

Because the ac Stark shift is *not* a resonance effect, the counter-rotating terms ignored by the RWA would add to S_1 and S_2 as[31,32]

$$S_1'=S_1+\sum_j|\Omega_{jp}|^2/(\omega_p+\omega_{j1}) \tag{A9a}$$

$$S_2'=S_2+\sum_j|\Omega_{jS}|^2/(\omega_S+\omega_{j2})\ . \tag{A9b}$$

Power broadening due to the Rabi oscillations *is* a resonance effect, and hence the RWA result for R is sufficient. By transforming the $C_{1,2}(t)$ amplitudes as

$$\tilde{C}_{1,2}(t)=C_{1,2}(t)e^{iS_{1,2}'t}\ ,$$

we finally obtain the effective two-level atom equations

$$\frac{\partial\tilde{C}_1(t)}{\partial t}=-iR\tilde{C}_2(t)e^{i\bar{\Delta}t}\ , \tag{A10a}$$

$$\frac{\partial\tilde{C}_2(t)}{\partial t}=-iR^*\tilde{C}_1(t)e^{-i\bar{\Delta}t}\ , \tag{A10b}$$

with $\bar{\Delta}=\Delta+S_1'-S_2'$. This set of equations is straightforwardly solved to give

$$C_1(t)e^{-i(\bar{\Delta}/2-S_1')t}=C_{10}\cos(\bar{R}t)-\frac{i}{\bar{R}}\left[\frac{\bar{\Delta}}{2}C_{10}+RC_{20}\right]\sin(\bar{R}t)\ , \tag{A11a}$$

$$C_2(t)e^{-i(\bar{\Delta}/2-S_2')t}=C_{20}\cos(\bar{R}t)-\frac{i}{\bar{R}}\left[\frac{\bar{\Delta}}{2}C_{20}+R^*C_{10}\right]\sin(\bar{R}t)\ , \tag{A11b}$$

where $C_{i0}=C_i(0)$ ($i=1,2$) and $\bar{R}=(|R|^2+\bar{\Delta}^2/4)^{1/2}$.

The population inversion for n photons in mode p and m photons in mode S is (letting C_{i0} and R be real quantities)

$$w_{nm}(t)=P_p(n)P_S(m)[|C_2(t)|^2-|C_1(t)|^2] \tag{A12a}$$

$$=P_p(n)P_S(m)\left[(C_{20}^2-C_{10}^2)\cos^2(\bar{R}t)+\left[\frac{\bar{\Delta}^2/4-R^2}{\bar{\Delta}^2/4+R^2}(C_{20}^2-C_{10}^2)-\frac{2\bar{\Delta}R}{\bar{\Delta}^2/4+R^2}C_{20}C_{10}\right]\sin^2(\bar{R}t)\right], \tag{A12b}$$

which for initial conditions $C_{10}=1$ and $C_{20}=0$ (i.e., the atom is initially in the ground state) reduces to

$$w_{nm}(t)\rightarrow P_p(n)P_S(m)\times\left[\frac{R^2-\bar{\Delta}^2/4}{R^2+\bar{\Delta}^2/4}\sin^2(\bar{R}t)-\cos^2(\bar{R}t)\right], \tag{A12c}$$

and for $\bar{\Delta}=0$ simplifies even further to

$$w_{nm}(t)\rightarrow P_p(n)P_S(m)[-\cos(2Rt)]\ . \tag{A12d}$$

To explicitly show the n,m dependence of $w_{nm}(t)$, we will introduce an interaction strength parameter λ through the equation

$$|R|^2=\left[\sum_j(\mathbf{d}_{1j}\cdot\boldsymbol{\epsilon}_p^*)(\mathbf{d}_{2j}\cdot\boldsymbol{\epsilon}_S)\frac{A_pA_S}{\Delta_j}\right]^2 n(m+1) \tag{A13a}$$

$$\equiv\lambda^2 n(m+1)\ . \tag{A13b}$$

Now, defining δ through the equation

$$\bar{\Delta}=2\lambda\delta\ , \tag{A14}$$

we may write (for $C_{10}=1$, $C_{20}=0$)

$$w_{nm}(t)=P_p(n)P_S(m)\times\left[\frac{n(m+1)-\delta^2}{n(m+1)+\delta^2}\sin^2\{[n(m+1)+\delta^2]^{1/2}\lambda t\}-\cos^2\{[n(m+1)+\delta^2]^{1/2}\lambda t\}\right]. \tag{A15}$$

The total population inversion is then given by

$$W(t)=\sum_{n,m}w_{nm}(t). \tag{A16}$$

APPENDIX B: DERIVATION OF THE PHENOMENOLOGICAL RAMAN HAMILTONIAN

The Hamiltonian in Eq. (A1) represents the total energy of the system shown in Fig. 1. However, phenomenologically one is tempted to look at the figure and simply write down in the rotating-wave approximation the Hamiltonian of Eq. (5) (with $\hbar=1$)

$$\hat{H}_{\text{phenom}}=\tfrac{1}{2}\omega_0\hat{\sigma}_z+\omega_p\hat{a}_p^\dagger\hat{a}_p+\omega_S\hat{a}_S^\dagger\hat{a}_S+\lambda(\hat{a}_p^\dagger\hat{a}_S\hat{\sigma}^-+\hat{a}_p\hat{a}_S^\dagger\hat{\sigma}^+)\ , \tag{B1}$$

where $\hat{\sigma}_z$ is the atomic inversion operator and $\hat{\sigma}^+$ ($\hat{\sigma}^-$) is the atomic raising (lowering) operator. This Hamiltonian represents the Raman interaction with $\hat{a}_p\hat{a}_S^\dagger\hat{\sigma}^+$ (absorb a pump photon, emit a Stokes photon, and the atom will rise from $|1\rangle$ to $|2\rangle$) plus $\hat{a}_p^\dagger\hat{a}_S\hat{\sigma}^-$ (emit a pump photon, absorb a Stokes photon, and move from $|2\rangle$ down to $|1\rangle$). How is this Hamiltonian related to the full Hamiltonian?

The free-atom energy is the easiest to obtain. With $\hat{\sigma}_z\equiv\hat{\sigma}_{22}-\hat{\sigma}_{11}$ and $\omega_0=\omega_2-\omega_1$, we may write immediately

$$\omega_1\hat{\sigma}_{11}+\omega_2\hat{\sigma}_{22}=\tfrac{1}{2}\omega_0\hat{\sigma}_z+\tfrac{1}{2}\omega_0(\hat{\sigma}_{11}+\hat{\sigma}_{22})\ . \tag{B2}$$

Since we assume population is conserved, $\hat{\sigma}_{11}+\hat{\sigma}_{22}$ is a constant (we are far enough off resonance with the $|j\rangle$ states that no population gets transferred to them so that $\sigma_{jj}=0$) and that term may be dropped (because the zero of energy is not a well-defined quantity). For the interaction energy, we will step into the Heisenberg picture and write the dynamical equation satisfied by the time-dependent transition operators $\hat{\sigma}_{ij}(t)$ (Ref. 34):

$$\dot{\hat{\sigma}}_{ij}(t)=i\omega_{ij}\hat{\sigma}_{ij}(t)-\sum_\alpha\tfrac{1}{2}A_\alpha\left[\sum_n\mathbf{d}_{jn}\cdot[\boldsymbol{\epsilon}_\alpha\hat{a}_\alpha(t)-\boldsymbol{\epsilon}_\alpha^*\hat{a}_\alpha^\dagger(t)]\hat{\sigma}_{in}(t)-\sum_m\mathbf{d}_{mi}\cdot[\boldsymbol{\epsilon}_\alpha\hat{a}_\alpha(t)-\boldsymbol{\epsilon}_\alpha^*\hat{a}_\alpha^\dagger(t)]\sigma_{mj}(t)\right] \tag{B3}$$

in the absence of damping. In terms of these operators, the interaction energy is

$$-\hat{\mathbf{d}}\cdot\hat{\mathbf{E}}=-\sum_j(\mathbf{d}_{1j}\hat{\sigma}_{1j}+\mathbf{d}_{2j}\hat{\sigma}_{2j}+\text{H.c.})\cdot i\sum_\alpha A_\alpha[\boldsymbol{\epsilon}_\alpha a_\alpha(t)-\boldsymbol{\epsilon}_\alpha^* a_\alpha^\dagger(t)]\ , \tag{B4}$$

which in the RWA reduces to

$$(-\hat{\mathbf{d}}\cdot\hat{\mathbf{E}})_{\text{RWA}}=iA_p\sum_j[\mathbf{d}_{j1}\cdot\boldsymbol{\epsilon}_p\hat{\sigma}_{j1}(t)\hat{a}_p(t)-\text{H.c.}]+iA_s\sum_j[\mathbf{d}_{j2}\cdot\boldsymbol{\epsilon}_S\hat{\sigma}_{j2}(t)\hat{a}_S(t)-\text{H.c.}]\ , \tag{B5}$$

where H.c. stands for Hermitian conjugate. Equation (B3) for $i=1$ becomes

$$\dot{\hat{\sigma}}_{1j}(t)\approx-i\omega_{j1}\hat{\sigma}_{1j}(t)-\tfrac{1}{2}A_p\{\mathbf{d}_{j1}\cdot[\boldsymbol{\epsilon}_p\hat{a}_p(t)-\text{H.c.}]\hat{\sigma}_{11}(t)+\mathbf{d}_{j2}\cdot[\boldsymbol{\epsilon}_p\hat{a}_p(t)-\text{H.c.}]\hat{\sigma}_{12}(t)\}-\tfrac{1}{2}A_S\{\mathbf{d}_{j1}\cdot[\boldsymbol{\epsilon}_S\hat{a}_S(t)-\text{H.c.}]\hat{\sigma}_{11}(t)+\mathbf{d}_{j2}\cdot[\boldsymbol{\epsilon}_S\hat{a}_S(t)-\text{H.c.}]\hat{\sigma}_{12}(t)\}\ , \tag{B6}$$

where we have dropped terms containing $\sigma_{jj'}(t)$ since we are far off resonance with the $|j\rangle$ states and do not expect any real transitions to occur to or between them. Now, if we make the following substitutions in Eq. (B6):

$$\hat{a}_p(t)=\tilde{a}_p e^{-i\omega_p t}, \tag{B7a}$$

$$\hat{\sigma}_{1j}(t)=\tilde{\sigma}_{1j} e^{-i\omega_p t}, \tag{B7b}$$

$$\hat{\sigma}_{12}(t)=\tilde{\sigma}_{12} e^{-i\omega_{21} t}, \tag{B7c}$$

and drop all rapidly oscillating terms (as per the RWA), we find

$$\dot{\tilde{\sigma}}_{1j}(t)\approx i\Delta_j\tilde{\sigma}_{1j}-\tfrac{1}{2}A_p\cdot\mathbf{d}_{j1}\cdot\boldsymbol{\epsilon}_p\tilde{a}_p\hat{\sigma}_{11} -\tfrac{1}{2}A_S\mathbf{d}_{j2}\cdot\boldsymbol{\epsilon}_S\tilde{a}_S\tilde{\sigma}_{12}e^{i\Delta t}. \tag{B8}$$

If we use the method of adiabatic elimination on this equation[12,31–33] (as in Appendix A) and then go back to the original variables, we get

$$\hat{\sigma}_{1j}(t)\approx -i\frac{1}{2\Delta_j}A_p\mathbf{d}_{j1}\cdot\boldsymbol{\epsilon}_p\hat{a}_p(t)\hat{\sigma}_{11}(t) -i\frac{1}{2\Delta_j}A_S\mathbf{d}_{j2}\cdot\boldsymbol{\epsilon}_S\hat{a}_S(t)\hat{\sigma}_{12}(t). \tag{B9}$$

Substituting this into the RWA interaction energy of Eq. (B4) yields

$$(-\hat{\mathbf{d}}\cdot\hat{\mathbf{E}})_{\mathrm{RWA}}\approx\tfrac{1}{2}\lambda_p(\hat{a}_p\hat{a}_p^{\dagger}+\hat{a}_p^{\dagger}\hat{a}_p)\hat{\sigma}_{11} +\tfrac{1}{2}\lambda_S(\hat{a}_S\hat{a}_S^{\dagger}+\hat{a}_S^{\dagger}\hat{a}_S)\hat{\sigma}_{22} +\lambda\hat{a}_p^{\dagger}\hat{a}_S\hat{\sigma}_{12}+\lambda^*\hat{a}_p\hat{a}_S^{\dagger}\hat{\sigma}_{21}. \tag{B10}$$

The first two terms will give rise to the Stark shifts of levels $|1\rangle$ and $|2\rangle$. If we ignore the Stark shifts and let $\mathbf{d}_{ij}=\mathbf{d}_{ji}$ and $\boldsymbol{\epsilon}_\alpha^*=\boldsymbol{\epsilon}_\alpha$, then we will obtain Eq. (B1) [or equivalently Eq. (5)] since $\sigma_{21}=\hat{\sigma}^+$ and $\hat{\sigma}_{12}=\hat{\sigma}^-$.

*Also at: Department of Physics, University of New Mexico, Albuquerque, NM 87131.

[1]E. T. Jaynes and F. W. Cummings, Proc. IEEE **51**, 89 (1963).
[2]H. L. Yoo and J. H. Eberly, Phys. Rep. **118**, 239 (1985).
[3]S. M. Barnett, P. Filipowicz, J. Javanainen, P. L. Knight, and P. Meystre, in *Frontiers of Quantum Optics,* edited by E. R. Pike and S. Sarkar (Hilger, Bristol, 1986), pp. 485–520.
[4]S. J. D. Phoenix and P. L. Knight, Ann. Phys. (N.Y.) **186**, 381 (1988).
[5]R. J. Glauber, Phys. Rev. **130**, 2529 (1963); **131**, 2766 (1963).
[6]L. Allen and J. H. Eberly, *Optical Resonance and Two-Level Atoms* (Wiley, New York, 1975).
[7]J. H. Eberly, N. B. Narozhny, and J. J. Sanchez-Mondragon, Phys. Rev. Lett. **44**, 1323 (1980); N. B. Narozhny, J. J. Sanchez-Mondragon, and J. H. Eberly, Phys. Rev. A **23**, 236 (1981); H. L. Yoo, J. J. Sanchez-Mondragon, and J. H. Eberly, J. Phys. B **14**, 1383 (1981).
[8]B. Buck and C. V. Sukumar, Phys. Lett. **81A**, 132 (1981).
[9]C. V. Sukumar and B. Buck, Phys. Lett. **83A**, 211 (1981).
[10]B. Buck and C. V. Sukumar, J. Phys. A **17**, 877 (1984); C. V. Sukumar and B. Buck, J. Phys. A **17**, 885 (1984).
[11]S. Singh, Phys. Rev. A **25**, 3206 (1982).
[12]P. Alsing and M. S. Zubairy, J. Opt. Soc. Am. B **4**, 177 (1987); R. R. Puri and R. K. Bullough, *ibid.* **5**, 2021 (1988).
[13]E. A. Kochetov, J. Phys. A **20**, 2433 (1987).
[14]S.-C. Gou, Phys. Rev. A **40**, 5116 (1989).
[15]M. S. Abdalla, M. M. A. Ahmed, and A.-S. F. Obada, Physica A **162**, 215 (1990).
[16]S. J. D. Phoenix and P. L. Knight, J. Opt. Soc. Am. **7**, 116 (1990).
[17]D. A. Cardimona, M. P. Sharma, and M. A. Ortega, J. Phys. B **22**, 4029 (1989).
[18]D. A. Cardimona, Phys. Rev. A **41**, 5016 (1990).
[19]S. M. Barnett and P. L. Knight, Opt. Acta **31**, 435 (1984); **31**, 1203 (1984); Z. Deng, Opt. Commun. **54**, 222 (1985); S. Mahmood and M. S. Zubairy, Phys. Rev. A **35**, 425 (1987); M. S. Iqbal, S. Mahmood, M. S. K. Razmi, and M. S. Zubairy, J. Opt. Soc. Am. B **5**, 1312 (1988).
[20]M. P. Sharma, D. A. Cardimona, and A. Gavrielides, Opt. Commun. **72**, 291 (1989); M. P. Sharma, D. A. Cardimona, and A. Garvielides, J. Opt. Soc. Am. B **6**, 1942 (1989).
[21]S. M. Barnett and P. L. Knight, Phys. Rev. A **33**, 2444 (1986); R. R. Puri and G. S. Agarwal, *ibid.* **33**, 3610 (1986); **35**, 3433 (1987).
[22]P. Goy, J. M. Raimond, M. Gross, and S. Haroche, Phys. Rev. Lett. **50**, 1903 (1983); D. Meshede, H. Walther, and G. Muller, *ibid.* **54**, 551 (1985).
[23]M. Brune, J. M. Raimond, and S. Haroche, Phys. Rev. A **35**, 154 (1987), and references therein.
[24]I. Ashraf and M. S. Zubairy, Opt. Commun. **77**, 85 (1990).
[25]M. Brune, J. M. Raimond, P. Goy, L. Davidovich, and S. Haroche, Phys. Rev. Lett. **59**, 1899 (1987).
[26]G. Rempe, H. Walther, and N. Klein, Phys. Rev. Lett. **58**, 353 (1987).
[27]P. L. Knight and P. M. Radmore, Phys. Rev. A **26**, 676 (1982).
[28]V. Buzek, Phys. Rev. A **39**, 3196 (1989); L. Schoendroff and H. Risken, *ibid.* **41**, 5147 (1990); M. Chaichian, D. Ellinas, and P. P. Kulish, Phys. Rev. Lett. **65**, 980 (1990).
[29]H. A. Bethe and E. E. Salpeter, *Quantum Mechanics of One- and Two-Electron Atoms* (Plenum, New York, 1957).
[30]V. Kovanis, M. P. Sharma, and D. A. Cardimona (unpublished); D. A. Cardimona, V. Kovanis, and M. P. Sharma, in *Optical Society of America Annual Meeting Technical Digest 1990* (Optical Society of America, Washington, D.C., 1990), Vol. 15, p. 66.
[31]P. Alsing, P. R. Peterson, D. A. Cardimona, and A. Gavrielides, IEEE J. Quantum Electron. **QE-23**, 557 (1987).
[32]L. Allen and C. R. Stroud, Jr., Phys. Rep. **91**, 1 (1982).
[33]D. A Cardimona, M. P. Sharma, and A. Gavrielides, J. Mod. Opt. **37**, 1593 (1990).
[34]P. W. Milonni, Phys. Rep. C **25**, 1 (1976).